

Ovis aries Papillomavirus 3 in Ovine Cutaneous Squamous Cell Carcinoma

Veterinary Pathology
1-8
© The Author(s) 2017
Reprints and permission:
sagepub.com/journalsPermissions.nav
DOI: 10.1177/0300985817705171
journals.sagepub.com/home/vet



Veronica Vitiello¹, Giovanni P. Burrari¹, Mariagrazia Agus¹,
Antonio G. Anfossi¹, Alberto Alberti¹, Elisabetta Antuofermo¹,
Stefano Rocca¹, Tiziana Cubeddu¹, and Salvatore Pirino¹

Abstract

Squamous cell carcinoma (SCC) is a common malignancy affecting humans and other animals. Papillomaviruses (PVs) are frequently reported as causal agents of cutaneous benign and malignant epithelial lesions in different animal species, but only few studies have investigated their role in ovine SCC. In this study, we explore the possible involvement of the *Ovis aries* PVs (OaPV1, OaPV2, OaPV3) in cutaneous SCC using an integrated histological and molecular approach. Forty cutaneous SCCs from different anatomical locations of Sardinian sheep and 40 matched non-SCC samples were evaluated histologically and by polymerase chain reaction (PCR) to assess the presence of ovine PVs. In addition, DNA in situ hybridization (ISH) and reverse transcription–polymerase chain reaction (RT-PCR) were carried out to evaluate the cellular localization and viral transcriptional activity, respectively. OaPV3 DNA was detected in 26 of 40 (65%) SCCs and in 12 of 40 (30%) non-SCC samples using PCR. OaPV1 and OaPV2 were not detected. OaPV3 viral DNA was observed by ISH in malignant epithelial squamous cells of 18 of 40 (45%) SCCs. In addition, the viral transcriptional activity was identified in 24 of 40 (60%) SCCs by RT-PCR. Notably, a higher viral positivity was observed in SCCs compared with non-SCC samples. The considerable infection rate of OaPV3 in the most common skin tumor of the sheep suggests that PV could represent a key factor in the onset of ovine SCC.

Keywords

in situ hybridization, ovine, papillomavirus, neoplasia, skin, sheep, squamous cell carcinoma

Papillomaviruses (PVs; family Papillomaviridae) are highly species-specific viruses able to infect mammals, birds, and reptile species.⁴² PVs are small and nonenveloped viruses with a highly conserved circular double-stranded DNA genome of approximately 8 kb in length.^{18,38} Most PVs infect the basal layer of the stratified epithelium and replicate exclusively in epithelial cells, with a life cycle tightly regulated by cellular differentiation.^{13,22,31,32} Moreover, a small number of PVs infect and transform fibroblast cells.²⁴ The epithelial infection usually begins from cutaneous or mucosal surface lesions and results in benign proliferative lesions or, rarely, malignant cancers.^{20,21,42}

In animals, 112 PV types distributed over 32 genera have been characterized based on their well-conserved L1 nucleotide sequence.^{7,18,38} In sheep (*Ovis aries*), 2 PVs, named *Ovis aries* papillomavirus 1 (OaPV1) and 2 (OaPV2), have been described in Australia and classified into the *Delta* genus. These viruses are associated with cutaneous fibropapillomas, although their viral activity in benign lesions has been poorly investigated in sheep. In cows, bovine PVs of the *Delta* genus are responsible for cutaneous fibropapillomas, which spontaneously regress in immunocompetent animals but can potentially progress to squamous cell carcinoma (SCC) in the presence of co-carcinogenic factors.^{9,11,36}

Recently, in Sardinia (Italy), a novel epidermotropic ovine PV, *Ovis aries* papillomavirus 3 (OaPV3), has been described in 2 ovine SCCs.³

The genomic characterization of OaPV3 (GenBank accession no. FJ796965) showed a low degree of similarity (less than 60%) with other PVs and was placed in the genus *Dyokappa*. Unlike the *Delta* papillomavirus, the OaPV3 genome lacks the E5 gene and retains the conserved retinoblastoma tumor suppressor binding sequence motif in E7, suggesting that this virus could play a key role in malignant cancer development.^{3,19}

SCC, a malignant tumor of epithelial origin with differentiation to keratinocytes, is widely described in animals and is the most common form of skin cancer in sheep.^{3,29} The cause of

¹Department of Veterinary Medicine, Sassari University, Sassari, Italy

Supplemental material for this article is available on the *Veterinary Pathology* website at <http://journals.sagepub.com/doi/suppl/10.1177/0300985817705171>.

Corresponding Author:

Salvatore Pirino, Department of Veterinary Medicine, Sassari University, Via Vienna 2, 07100 Sassari, Italy.
Email: pirino@uniss.it

this neoplasm appears to be multifactorial, although prolonged exposure to ultraviolet radiation and poor skin pigmentation are considered primary risk factors for tumor development.^{1,27–29}

However, oncogenic viruses, such as PVs, seem to be associated with the cutaneous SCC development in human and animal species, suggesting a possible correlation between the infection and carcinoma.^{4,33,41} The aim of this study was to investigate the presence of OaPV1, OaPV2, and OaPV3 in SCC samples of Sardinian sheep by histological and biomolecular analysis.

Materials and Methods

Origin of the Samples

Forty cutaneous SCC and 40 matched non-SCC samples from 70 sheep of the Sardinian breed, obtained from udder (SCC = 21; non-SCC = 21), eyelid (SCC = 7; non-SCC = 7), pinnae (SCC = 5; non-SCC = 5), planum nasale (SCC = 4; non-SCC = 4), and trunk (SCC = 3; non-SCC = 3), were fixed in 10% neutral buffered formalin and then paraffin embedded (FFPE). Tissue sections (3 µm thick) from both SCC and non-SCC samples were stained with hematoxylin and eosin (HE) for histopathological evaluation, and 10 serial sections from each FFPE sample were collected in a 1.5-ml tube and used for DNA and RNA isolation. In addition, FFPE SCC samples were used for in situ hybridization (ISH).

Histopathology

Tumors were classified according to World Health Organization criteria for tumors of the skin and soft tissue and graded according to a semiquantitative scheme, originally developed for oral SCC in dogs, with minor modifications.^{6,30} Degree of keratinization, nuclear pleomorphism, number of mitoses, pattern of invasion, and lymphoplasmacytic infiltration were each assigned a score ranging from 1 to 4 points. Histopathological features were evaluated in 10 high-power fields (HPF), and the sum of each parameter subclassified SCCs as follows: grade 1 or well differentiated (WDC), 1 to 7 points; grade 2 or moderately differentiated (MDC), 8 to 14 points; and grade 3 or poorly differentiated (PDC), 15 to 20 points. The stained slides were reviewed independently by 3 pathologists (G.P.B., E.A., and S.P.), and a consensus score was obtained for each case on a multiheaded microscope. Digital computer images were recorded with a Nikon (Tokyo, Japan) Ds-fi1 camera.

Detection of Ovine PVs

DNA from SCC and non-SCC FFPE samples was extracted using the AllPrep DNA/RNA FFPE kit (Qiagen, Milano, Italy), following the manufacturer's instructions.

The quality of the DNA samples was checked by polymerase chain reaction (PCR) amplification of the ovine glyceraldehyde 3-phosphate dehydrogenase (GAPDH) gene.¹⁴ The amplification program consisted of an initial denaturation step at 94°C for 5 minutes, followed by 30 thermal cycles at 94°C

Table 1. Primer Sequences for Polymerase Chain Reaction.

Primer	Sequence (5'–3' orientation)	Product Size, bp
LI OaPV1 FP	CGCCCGTCTCCCTACGGTGC	177
LI OaPV1 RP	CTGCAACGCCTCCGGACCCC	
LI OaPV2 FP	CGCACCACAGCCCAAGGCAC	147
LI OaPV2 RP	TCCAGCGTCCACACGGTCTGA	
LI OaPV3 FP	AACTGGACTTGTCTTCCATG	127
LI OaPV3 RP	AAAGACTCGGTATTGGGAGG	

bp, base pairs; FP, forward primer; OaPV, *Ovis aries* papillomavirus; RP, reverse primer.

for 30 seconds, 60°C for 30 seconds, and 72°C for 30 seconds, with a final elongation step at 72°C for 5 minutes.

Subsequently, to evaluate the presence of ovine PVs (OaPV1, OaPV2, OaPV3) in both SCCs and non-SCC samples, 3 distinct PCR assays for detection of the L1 gene were performed in a total volume of 50 µl containing 1.5 mM MgCl₂, 0.2 µM of each oligonucleotide primer, 0.2 mM of each dNTP, 0.62 U Taq DNA polymerase (Qiagen), and 2.5 µl DNA.

Each reaction was carried out using primers set listed in Table 1. Reaction conditions for OaPV1 and OaPV2 included initial denaturation at 95°C for 5 minutes, followed by 40 cycles at 95°C for 30 seconds, annealing at 56°C for 30 seconds, and extension at 72°C for 30 seconds, with a final elongation step at 72°C for 5 minutes. The same conditions were maintained for the OaPV3, except for the annealing temperature at 57°C.³

In OaPV3 reactions, a negative control (purified PCR-grade water) and a positive control (OaPV3 DNA cloned into pUC19) were included.³ PCRs were repeated 3 times and the amplified products were visualized after electrophoresis in 2% agarose gel run containing GelRed Nucleic Acid Gel Stain (Biotium, Hayward, CA) in TAE 1× buffer (40 mM Tris, 1 mM Na₂EDTA, 20 mM acetic acid), at 5 mVcm⁻¹ for 90 minutes.

DNA In Situ Hybridization for OaPV3 Localization in SCCs

To localize OaPV3 DNA in SCC samples, 2 digoxigenin-labeled and unlabeled probes have been generated by using the PCR DIG Probe Synthesis Kit (Roche, Milano, Italy), following the manufacturer's instructions. Specifically, a 151-base pair (bp) E6 DNA probe and a 127-bp L1 DNA probe were generated as previously described and used for colorimetric and fluorescence ISH experiments.³

A negative control (ovine liver) and a positive control (OaPV3 ISH-positive SCC sample³) were included in each experiment. Briefly, deparaffinized and rehydrated tissue sections were placed in Tris-buffered saline (TBS) at 37°C for 5 minutes, treated with 0.8% pepsin in HCl 0.2 N at 37°C for 30 minutes, and rinsed in TBS. Subsequently, a postfixation step was performed by dehydration in increasing concentrations of ethanol, from 70% v/v to 100%, and air-dried. Samples were treated with prehybridization solution (50% molecular-grade hybridization solution II [Fluka Chimica, Milano, Italy], 43%

formamide, 7% mQ water) at 37°C for 1 hour and then at 95°C for 8 minutes and at 37°C overnight with the hybridization solution containing the denatured DNA probe (50% molecular-grade hybridization solution II [Fluka Chimica], 43% formamide, 6.5% of water, and 10 ng/ml E6 or L1 probes). Subsequently, sections were washed in decreasing concentration of molecular biology-grade SSPE (Sigma-Aldrich, Milano, Italy; 2×, 1×, 0.5× SSPE and 0.1× SSPE + bovine serum albumin 0.2%) to remove the unbound probes. After incubation for 1 hour in blocking solution (2% normal rat serum, 0.3% Triton X-100, and Tris-HCl [pH 8.2]), sections were incubated at 25°C for 1 hour with anti-digoxigenin-AP Fab fragments (Sigma-Aldrich) diluted 1:200.

Color development was performed incubating sections at 37°C for 50 minutes with detection buffer (Tris-HCl 1 M, NaCl 5 M, MgCl₂ 1 M [pH 9.5]) containing 2% 5-bromo-4-chloro-3-indolylphosphate and 2% 4-nitro blue tetrazolium chloride. After washing in mQ water, sections were closed with a coverslip using Top-Water mount (Sigma-Aldrich).

Fluorescence-developed sections were incubated in the dark at 25°C for 45 minutes with the Vector Red Alkaline Phosphatase Substrate Kit (Vector Laboratories, Burlingame, CA). After washing in mQ water, nuclei were counterstained with Hoechst diluted 1:1000, and then sections were closed with Top-Water mount (Sigma-Aldrich). Finally, slides were observed in a Leica TCS SP5 confocal microscope (Leica Microsystems, Wetzlar, Germany), and the LAS AF Lite (Leica Microsystems) software was used for image processing.

The extent of colorimetric hybridization signal was evaluated based upon the brown nuclear signal and semiquantitatively scored according to the number of positive cells in 10 high-power fields (400×) (grade 0: no positive cells; 1: 10%–40%; 2: 41%–70%; 3: >70%).

Detection of OaPV3 Early and Late Transcripts in SCCs

RNA from FFPE samples was extracted using the AllPrep DNA/RNA FFPE kit (Qiagen). Reverse transcription–polymerase chain reaction (RT-PCR) was performed using a 2-step protocol. RNA was reverse transcribed (iScript cDNA Synthesis kit; Bio-Rad, Segrate, Italy) following the manufacturer's instructions. PCR assays were conducted to detect OaPV3 early (E6) and late (L1) transcripts and for the ovine GAPDH gene to assess complementary DNA (cDNA) quality.^{3,14} In each reverse transcription and amplification reaction, a negative control (purified PCR-grade water) and a positive control (OaPV3 RNA isolated from SCC tissue³) were included. RT-PCRs were performed in a 50-μl master mix containing 1.5 mM MgCl₂, 0.2 μM of each oligonucleotide primer, 0.2 mM of each dNTP, 0.62 U Taq DNA polymerase (Qiagen), and 2.5 μl cDNA.

Cycling conditions for E6 primers included initial denaturation at 95°C for 5 minutes, followed by 40 cycles at 95°C for 30 seconds, annealing at 52°C for 30 seconds, and extension at 72°C for 30 seconds, with a final elongation step at 72°C for 5

minutes. Reaction conditions were maintained for L1 primers, except for the annealing temperature at 57°C.

RT-PCR results were visualized on 2% agarose gel containing GelRed Nucleic Acid Gel Stain (Biotium) after a run of 90 minutes in an electric field of 5 mVcm⁻¹ in TAE 1× buffer.

A representative subset of amplified products positive for both OaPV3 E6 and the L1 target was purified using the QIAquick Gel Extraction Kit (Qiagen) and directly sequenced using the ABI Prism 3100 Genetic Analyzer (Applied Biosystems, Monza, Italy). Sequenced fragments were analyzed by BLAST search of the NCBI GenBank database.

Statistical Analysis

Statistical analyses were performed using Stata 11.2 software (StataCorp LP, College Station, TX).

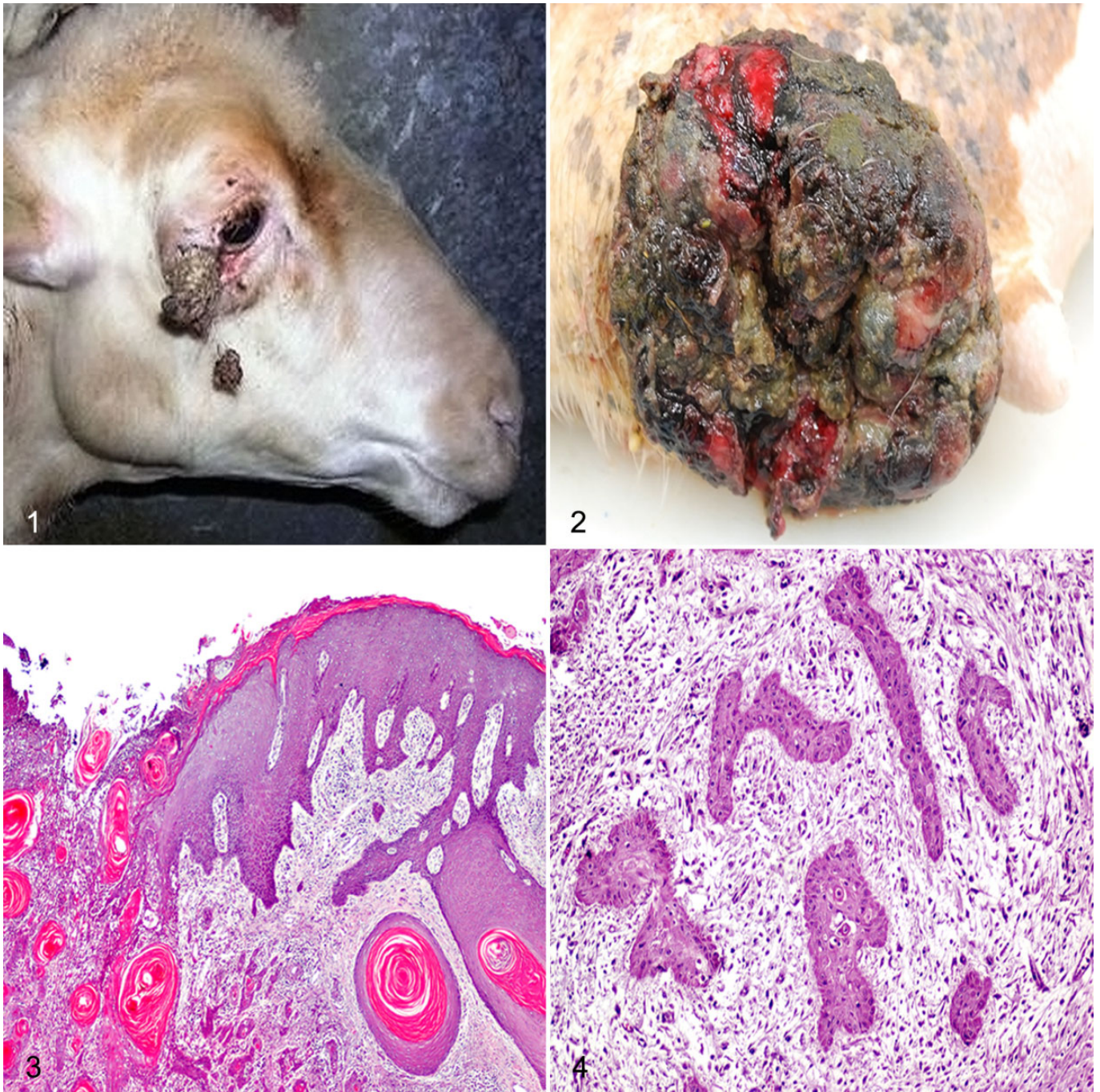
After performing descriptive statistics, categorical and ordinal variables were evaluated by Spearman ρ correlation coefficient, with Bonferroni adjustment and χ^2 test or Fisher's exact test. In particular, Spearman rank correlation was performed to assess the usefulness of the modified Anneroth's grading scheme in the histological evaluation of ovine SCC. A value of ρ approximately equal to 1 indicates a good correlation, a value near 0 indicates a poor correlation, and a negative value indicates an inverse correlation. The χ^2 or Fisher's exact test was performed to assess the differences in PV presence in SCC and non-SCC samples, as well as the potential correlations between OaPV3 DNA presence in UV-exposed head regions (including eyelid, planum nasale, and pinnae lesions) in the 2-sample set. A *P* value <.05 was considered significant.

Results

Histopathology

Grossly, SCCs appeared as horns (Fig. 1) or cauliflower-like exophytic masses of variable size (from 4 to 9 cm) involving, in some cases, the dermal and subcutaneous structures and frequently with epidermal ulceration (Fig. 2). Histologically, SCCs were characterized by cuboidal to polyhedral epithelial cell proliferations arranged in cords, trabeculae, or islands. The majority of the examined neoplasms showed an orderly progression from polyhedral nonkeratinized cells localized at the periphery of the neoplastic epithelial islands to large polygonal keratinized cells.

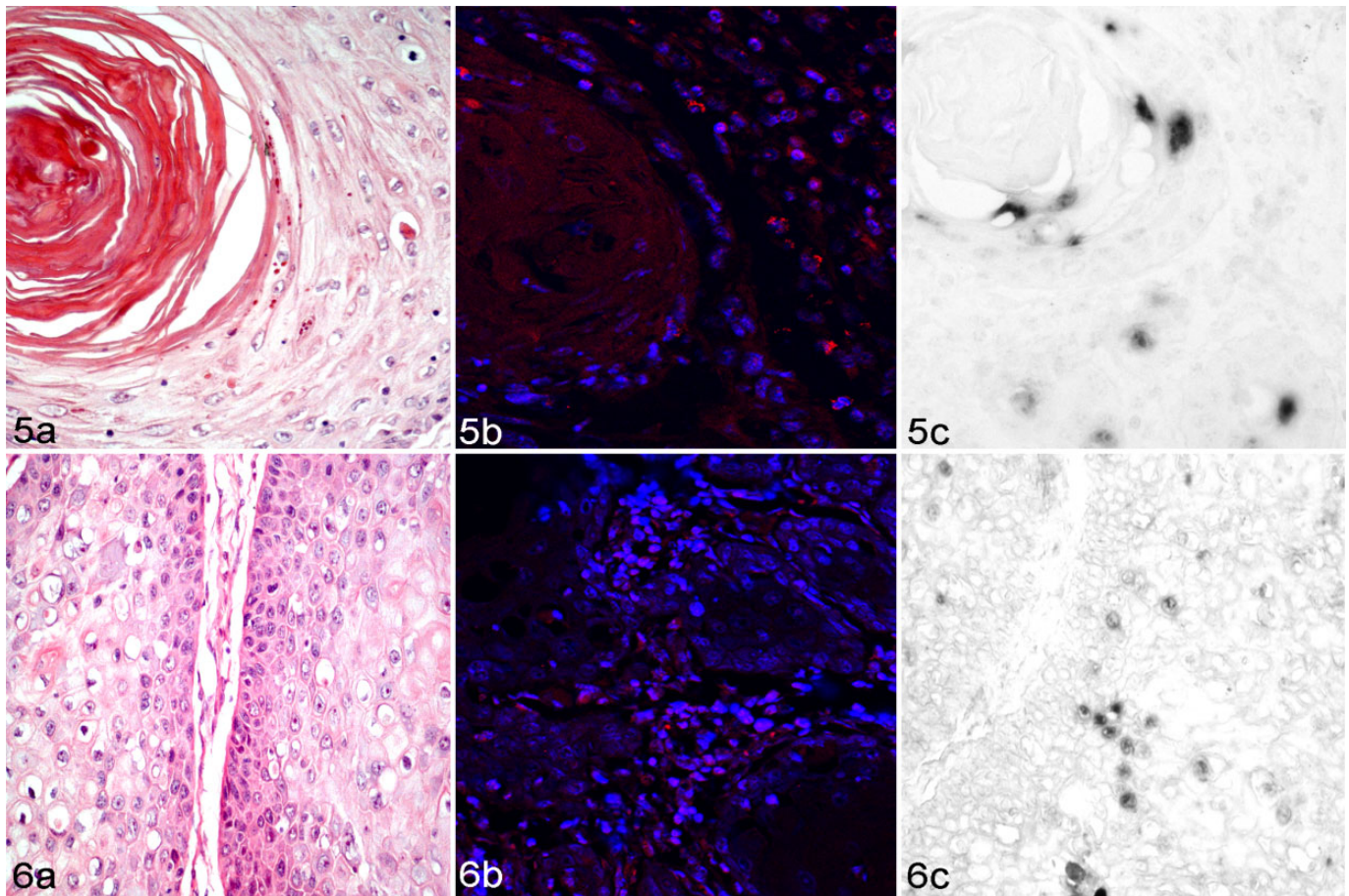
According to the modified Anneroth's multifactorial grading system, none of the SCC samples were well differentiated, whereas 36 of 40 (90%) SCCs localized in udder (*n* = 19), eyelid (*n* = 7), pinnae (*n* = 5), planum nasale (*n* = 3), and trunk (*n* = 2) were moderately differentiated (median, 11; range, 8–14) (Suppl. Table S1). Histologically, moderately differentiated SCCs were characterized by trabeculae or small islands of squamous cells associated with central eosinophilic keratin (keratin pearls) (Fig. 3). Neoplastic cells exhibited prominent intercellular bridges, abundant amphophilic to eosinophilic cytoplasm, and large, irregularly round to oval



Figures 1–4. Squamous cell carcinoma (SCC), sheep, skin. **Figures 1–2.** Horn and cauliflower-like gross appearance of SCC in the right eye (1) and in the udder (2). **Figure 3.** Moderately differentiated SCC, case No. 29. There are irregular cords of squamous cells with still-evident keratin pearls. Hematoxylin and eosin (HE). **Figure 4.** Poorly differentiated SCC, case No. 20. There are islands of pleomorphic neoplastic cells embedded in an edematous stroma. HE.

nuclei with finely stippled chromatin. Cells showed moderate anisocytosis and anisokaryosis and a variable number of mitoses ranging from 0 to 6 per HPF (1.52 ± 0.20 , mean \pm SEM). Furthermore, a mild to moderate lymphoplasmacytic infiltrate intermingled with keratin pearls was frequently observed.

In contrast, 4 of 40 (10%) SCCs obtained from udder ($n = 2$), planum nasale ($n = 1$), and trunk ($n = 1$) were poorly differentiated (median, 15; range, 15–20) (Suppl. Table S1) and characterized by neoplastic cells organized in trabeculae rather than islands, disseminated in small groups or in keratinized single cells, often with invasion of the dermis (Fig. 4). Cells



Figures 5–6. Squamous cell carcinoma (SCC), sheep, skin. **Figure 5.** Moderately differentiated SCC, case No. 2. Histological aspect of a keratin pearl (a), fluorescence (b), and colorimetric (c) *Ovis aries* papillomavirus 3 (OaPV3) hybridization signals in the nuclei of intermediate and superficial layers. HE (a), in situ hybridization (b, c) with E6 OaPV3 probe. **Figure 6.** Moderately differentiated SCC, case No. 29. An island of malignant squamous cells (a), with fluorescence (b) and colorimetric (c) hybridization signals in the nuclei. HE (a), in situ hybridization (b, c) with LI OaPV3 probe.

showed extreme nuclear pleomorphism, and the mitoses were atypical (1.5 ± 0.20 , mean \pm SEM). Furthermore, a moderate lymphoplasmacytic infiltrate, admixed with degenerated neutrophils, scattered necrotic areas, and stromal fibroplasia, was observed.

The superficial dermal collagen fibers of both SCC and non-SCC samples from eyelid, planum nasale, and pinnae appeared pale and hypocellular (moderate solar elastosis) and, in certain cases, were characterized by a mild degree of lamellar fibrosis. In addition, there was thickening of vessel walls with endothelial swelling and sometimes an obvious sclerotic change, often admixed with neutrophilic inflammation with a low number of lymphocytes, plasma cells, and macrophages.

By Spearman rank correlation, the degree of keratinization was inversely associated with both nuclear pleomorphism ($\rho = -0.2348$, $P < .001$) and number of mitoses ($\rho = -0.1195$, $P < .01$) while, as expected, pleomorphism was positively associated with number of mitoses ($\rho = 0.2106$, $P < .001$) and pattern of invasion ($\rho = 0.3853$, $P < .001$). No statistical association was observed between the anatomic localization of the neoplasms and the SCC grade ($\chi^2 = 4.15$, $P = .386$).

PCR Detection of Ovine PVs

OaPV3 DNA was amplified from 26 of 40 (65%) SCCs and 12 of 40 (30%) non-SCCs ($\chi^2 = 9.82$, $P = .002$; Suppl. Tables S1–S2). All examined samples tested negative for OaPV1 and OaPV2 DNA but were positive for the GAPDH gene. OaPV3 DNA was shown in 25 of 36 (69%) moderately differentiated SCCs localized in udder ($n = 12$), eyelid ($n = 3$), pinnae ($n = 5$), planum nasale ($n = 3$), and trunk ($n = 2$) and in 1 of 4 (25%) poorly differentiated SCC in the planum nasale (Suppl. Table S1). Similarly, OaPV3 nucleic acid was detected in non-SCC samples from the udder ($n = 6$), eyelid ($n = 2$), planum nasale ($n = 2$), and pinna ($n = 1$) (Suppl. Table S2).

No statistical association was observed between the presence of OaPV3 and the SCC histological pattern (Fisher's exact = 0.139, $P > .05$) or between PV infection and the location of the SCC (Fisher's exact = 0.109, $P > .05$). Conversely, a higher OaPV3 positivity was observed in SCC samples from UV-exposed regions of the head (including eyelid, planum nasale, and pinnae lesions) compared with non-SCC samples from these regions ($\chi^2 = 6.14$, $P = .013$).

Detection of OaPV3 in SCC by In Situ Hybridization

OaPV3 DNA was detected in 18 of 40 (45%) SCCs by colorimetric and fluorescence ISH. Specifically, the viral DNA was observed in 18 of 36 (50%) moderately differentiated SCCs from the udder ($n = 6$), pinnae ($n = 4$), eyelid ($n = 3$), planum nasale ($n = 3$), and trunk ($n = 2$) (Figs. 5, 6; Suppl. Table S1). No viral DNA was detected in poorly differentiated SCCs (0/4) and in negative control slides.

Sixteen of 18 (88%) positive slides were scored as grade 1 (10%–40% of positive cells), whereas 2 of 18 (11%) were scored as grade 2 (41%–70% of positive cells) (Suppl. Table S3).

Moderately differentiated SCCs demonstrated strong and diffuse nuclear hybridization signals in malignant squamous cells mostly in the basal and intermediate and, less frequently, in the superficial layers of keratin pearls (Figs. 5, 6). In addition, a hybridization signal was detected in the hair follicular epithelium of 1 sample (case No. 29, Suppl. Table S1).

Detection of OaPV3 Early and Late Transcripts in SCCs

OaPV3 early and late gene expression was detected by RT-PCR in 24 of 40 (60%) carcinomas (Suppl. Table S1). The presence of OaPV3 RNA, by RT-PCR, was identified in 23 of 36 (63%) moderately differentiated SCCs located in udder ($n = 10$), pinnae ($n = 5$), eyelid ($n = 3$), planum nasale ($n = 3$), and trunk ($n = 2$) and in 1 of 4 (25%) poorly differentiated SCCs, sampled in planum nasale ($n = 1$) (Suppl. Table S1). Specifically, 7 of 36 (19%) moderately differentiated SCCs revealed expression of both E6 and L1 genes, while 6 of 36 (16%) and 11 of 36 (30%) moderately differentiated SCCs revealed expression of only E6 or L1 transcripts, respectively. Finally, the poorly differentiated SCC exhibited only expression of the L1 gene (Suppl. Table S1). Amplification of the GAPDH gene was shown in all analyzed samples. The nucleotide BLAST search of the sequences confirmed a 100% identity for E6 and L1 OaPV3 transcripts.

Overall, PCR detected OaPV3 DNA in 26 of 40 (65%) SCCs, while RT-PCR revealed the presence of cDNA in 24 of 40 (60%) SCCs. Notably, these 2 RT-PCR negative samples (case Nos. 1 and 5, Suppl. Table S1) were OaPV3 positive by both PCR and ISH.

Discussion

In this report, we evaluated the presence of ovine PV DNA within SCC and non-SCC samples by PCR using specific primers for OaPV1, OaPV2, and OaPV3. As result, a high prevalence of OaPV3 DNA (65%) was identified in SCCs of Sardinian sheep. Furthermore, as previously reported, a lower prevalence (30%) of OaPV3 DNA in non-SCC samples was also observed, suggesting a possible etiological role for the virus in the tumor onset as proposed in humans.^{3,16} Conversely, none of the tested samples showed the presence of OaPV1 or

OaPV2 DNA. This could be related to the genome organization of these viruses. In fact, OaPV1 and OaPV2 encode the E5 hydrophobic transmembrane protein, a well-characterized protein in bovine PV1 with a strong transforming activity in fibroblasts.⁹ For this reason, and considering also the high sequence homology between the E5 genes of the *Delta* genus PV types, we could speculate that OaPV1 and OaPV2 are involved only in fibropapilloma tumor development.¹¹ Conversely, OaPV3 shows an epithelial tropism and lacks the E5 gene but retains E6 and E7 protein, involved in several functions such as anoikis, invasion, and altered functions of the p53 oncoprotein.^{3,17,34,35} In addition, OaPV-3 encodes the conserved retinoblastoma (Rb) tumor suppressor binding sequence motif in E7 that, as reported by Munger et al³⁴ and Bourgo et al,¹² promotes uncontrolled cell division by forming stable complexes with the Rb codified protein. These data, as well as the higher amplification rate in SCC samples compared with non-SCC samples, suggest that OaPV3 may play a preferential key role in epithelial malignant tumor development.

OaPV3-specific nuclear signal was detected in 45% of ovine SCCs by ISH technique. Even though PCR, as expected, was more sensitive in the detection of OaPV3 DNA and indeed revealed higher positivity than ISH, ISH is advantageous for the localization and quantification of infected cells.²⁵

Colorimetric ISH was most useful to detect the virus in tumor cells, while the nuclear signals were more marked by fluorescence analysis compared with the colorimetric method. The localization of OaPV3 nucleic acid was revealed in malignant squamous epithelial cells, confirming the epithelial tropism of this PV.³

Furthermore, in 1 case (case No. 29), the virus was detected in hair follicle epithelium. This result is in agreement with previously and recently reported data that support the hypothesis that adnexa could represent an important site of entry of the virus and, consequently, a reservoir for many PV types.^{20,24,33} As previously suggested, additional and focused studies will be necessary to prove this hypothesis.²⁴

RT-PCR for early and late genes showed the OaPV3 transcriptional activity in 60% of SCCs, similar to reports in human and cattle.^{8,10,40} In addition, based on the gene expression pattern of early or late transcripts, RT-PCR showed different stages of the viral life cycle, corroborating the hypothesis of a productive infection in tumor cells.⁴³

Through the RT-PCR analysis, OaPV3 cDNA was found in 24 of 26 PCR-positive SCCs. Furthermore, the presence of viral DNA with the concomitant lack of transcriptional activity in 2 cases (case Nos. 1 and 5, despite amplification of the ovine GAPDH confirming RNA integrity) could indicate a silent PV infection.^{15,26} These results are in agreement with previously reported data in humans and cattle, in which the activated host immune system is able to restrict the PV infection in basal cells, leading to altered transcriptional activity, with the lack of E6 and L1 viral gene expression in immunocompetent animals.^{15,22,26,39}

Our results showed that the modified Anneroth's multifactorial grading system could be useful to characterize ovine

cutaneous SCC, as confirmed by the statistical and biological relationship between parameters such as cellular pleomorphism, number of mitoses, and degree of invasion. The prognostic value of this grading system needs to be confirmed by additional studies. The different grades of ovine SCC were unrelated to PV infection, suggesting (as proposed in humans) that PVs are not the only factors responsible for tumor onset.^{5,23} In particular, the higher OaPV3 positivity in SCC samples from the UV-exposed regions compared with matched non-SCC samples suggests that the virus could represent a synergic factor together with prolonged exposure to UV radiation and poor skin pigmentation in tumor development and onset.^{1,27–29} Likewise, as demonstrated by in vitro studies, the local UV immunosuppressive effect promotes cellular malignant transformation, stimulating the activity of PV and increasing the viral protein levels (ie, E6) able to suppress proapoptotic proteins.^{2,37}

This study reports the first investigation of OaPV3 infection in a large number of Sardinian sheep with SCC and offers new insight into the pathogenesis of SCC in small ruminants. Our data suggest a multifactorial etiology of cutaneous SCC.

Declaration of Conflicting Interests

The author(s) declared no potential conflicts of interest with respect to the research, authorship, and/or publication of this article.

Funding

The author(s) received the following financial support for the research, authorship, and/or publication of this article: This research has been partially financed by Fondo di Ateneo per la Ricerca - Uniss (F.A.R. 2011 Pirin - grant).

References

- Ahmed AF, Hassanein KMA. Ovine and caprine cutaneous and ocular neoplasms. *Small Rumin Res*. 2012;**106**(2–3):189–200.
- Akgul B, Cooke JC, Storey A. HPV-associated skin disease. *J Pathol*. 2006;**208**(2):165–175.
- Alberti A, Pirino S, Pintore F, et al. *Ovis aries* papillomavirus 3: a prototype of a novel genus in the family Papillomaviridae associated with ovine squamous cell carcinoma. *Virology*. 2010;**407**(2):352–359.
- Aldabagh B, Angeles JGC, Cardones AR, et al. Cutaneous squamous cell carcinoma and human papillomavirus: is there an association? *Dermatol Surg*. 2013;**39**(1):1–23.
- Ally MS, Tang JY, Arron ST. Cutaneous human papillomavirus infection and basal cell carcinoma of the skin. *J Invest Dermatol*. 2013;**133**(6):1456–1458.
- Anneroth G, Batsakis J, Luna M. Review of the literature and a recommended system of malignancy grading in oral squamous-cell carcinomas. *Scand J Dent Res*. 1987;**95**(3):229–249.
- Bernard HU, Burk RD, Chen Z, et al. Classification of papillomaviruses (PVs) based on 189 PV types and proposal of taxonomic amendments. *Virology*. 2010;**401**(1):70–79.
- Bishop JA, Ma XJ, Wang H, et al. Detection of transcriptionally active high-risk HPV in patients with head and neck squamous cell carcinoma as visualized by a novel E6/E7 mRNA in situ hybridization method. *Am J Surg Pathol*. 2012;**36**(12):1874–1882.
- Bocaneti F, Altamura G, Corteggio A, et al. Bovine papillomavirus: new insights into an old disease. *Transbound Emerg Dis*. 2016;**63**(1):14–23.
- Borzacchiello G, Iovane G, Marcante ML, et al. Presence of bovine papillomavirus type 2 DNA and expression of the viral oncoprotein E5 in naturally occurring urinary bladder tumors in cows. *J Gen Virol*. 2003;**84**(pt 11):2921–2926.
- Borzacchiello G, Roperto F. Bovine papillomaviruses, papillomas and cancer in cattle. *Vet Res*. 2008;**39**(5):45.
- Bourgo RJ, Braden WA, Wells SI, et al. Activation of the retinoblastoma tumor suppressor mediates cell cycle inhibition and cell death in specific cervical cancer cell lines. *Mol Carcinog*. 2009;**48**(1):45–55.
- Bravo IG, Felez-Sanchez M. Papillomaviruses: viral evolution, cancer and evolutionary medicine. *Evol Med Public Health*. 2015;**2015**(1):32–51.
- Budhia S, Haring LF, McConnell I, et al. Quantitation of ovine cytokine mRNA by real-time RT-PCR. *J Immunol Methods*. 2006;**309**(1–2):160–172.
- Campo MS, Jarrett WFH, Oneil W, et al. Latent papillomavirus infection in cattle. *Res Vet Sci*. 1994;**56**(2):151–157.
- Chen ACH, McMillan NAJ, Antonsson A. Human papillomavirus type spectrum in normal skin of individuals with or without a history of frequent sun exposure. *J Gen Virol*. 2008;**89**(pt 11):2891–2897.
- Corteggio A, Altamura G, Roperto F, et al. Bovine papillomavirus E5 and E7 oncoproteins in naturally occurring tumors: are two better than one? *Infect Agent Cancer*. 2013;**8**(1):1.
- de Villiers EM, Fauquet C, Broker TR, et al. Classification of papillomaviruses. *Virology*. 2004;**324**(1):17–27.
- DiMaio D, Petti LM. The E5 proteins. *Virology*. 2013;**445**(1–2):99–114.
- Doorbar J. Model systems of human papillomavirus-associated disease. *J Pathol*. 2016;**238**(2):166–179.
- Doorbar J, Quint W, Banks L, et al. The biology and life-cycle of human papillomaviruses. *Vaccine*. 2012;**30**(suppl 5):F55–F70.
- Doorbar J. The papillomavirus life cycle. *J Clin Virol*. 2005;**32**(suppl 1):S7–S15.
- Forslund O, Iftner T, Andersson K, et al. Cutaneous human papillomaviruses found in sun-exposed skin: beta-papillomavirus species 2 predominates in squamous cell carcinoma. *J Infect Dis*. 2007;**196**(6):876–883.
- Gaynor AM, Zhu KW, Cruz FN Jr, et al. Localization of bovine papillomavirus nucleic acid in equine sarcoids. *Vet Pathol*. 2016;**53**(3):567–573.
- Hayat MA. Polymerase chain reaction technology. In: Hayat MA, ed. *Immunohistochemistry and In Situ Hybridization of Human Carcinomas*. San Diego, CA: Academic Press; 2004:45–48.
- Maran A, Amella CA, Dilorenzo TP, et al. Human papillomavirus type-11 transcripts are present at low abundance in latently infected respiratory tissues. *Virology*. 1995;**212**(2):285–294.
- Markey AC. Etiology and pathogenesis of squamous cell carcinoma. *Clin Dermatol*. 1995;**13**(6):537–543.
- Marks R. Squamous cell carcinoma. *Lancet*. 1996;**347**(9003):735–738.
- Mendez A, Perez J, Ruiz-Villamor E, et al. Clinicopathological study of an outbreak of squamous cell carcinoma in sheep. *Vet Rec*. 1997;**141**(23):597–600.
- Misdorp W. *Histological Classification of Mammary Tumors of the Dog and the Cat*. Washington, DC: Armed Forces Institute of Pathology in cooperation with the American Registry of Pathology and the World Health Organization Collaborating Center for Worldwide Reference on Comparative Oncology; 1999.
- Mistry N, Wibom C, Evander M. Cutaneous and mucosal human papillomaviruses differ in net surface charge, potential impact on tropism. *Viol J*. 2008;**5**:118.
- Munday JS. Bovine and human papillomaviruses: a comparative review. *Vet Pathol*. 2014;**51**(6):1063–1075.
- Munday JS, Kiupel M. Papillomavirus-associated cutaneous neoplasia in mammals. *Vet Pathol*. 2010;**47**(2):254–264.
- Munger K, Werness BA, Dyson N, et al. Complex formation of human papillomavirus E7 proteins with the retinoblastoma tumor suppressor gene product. *EMBO J*. 1989;**8**(13):4099–4105.
- Narisawa-Saito M, Kiyono T. Basic mechanisms of high-risk human papillomavirus-induced carcinogenesis: roles of E6 and E7 proteins. *Cancer Sci*. 2007;**98**(10):1505–1511.
- Nasir L, Campo MS. Bovine papillomaviruses: their role in the aetiology of cutaneous tumors of bovids and equids. *Vet Dermatol*. 2008;**19**(5):243–254.

37. Purdie KJ, Pennington J, Proby CM, et al. The promoter of a novel human papillomavirus (HPV77) associated with skin cancer displays UV responsiveness, which is mediated through a consensus p53 binding sequence. *EMBO J*. 1999;**18**(19):5359–5369.
38. Rector A, Van Ranst M. Animal papillomaviruses. *Virology*. 2013;**445**(1–2):213–223.
39. Stubenrauch F, Laimins LA. Human papillomavirus life cycle: active and latent phases. *Semin Cancer Biol*. 1999;**9**(6):379–386.
40. Ukpo OC, Flanagan JJ, Ma XJ, et al. High-risk human papillomavirus E6/E7 mRNA detection by a novel in situ hybridization assay strongly correlates with p16 expression and patient outcomes in oropharyngeal squamous cell carcinoma. *Am J Surg Pathol*. 2011;**35**(9):1343–1350.
41. Wang J, Aldabagh B, Yu J, et al. Role of human papillomavirus in cutaneous squamous cell carcinoma: a meta-analysis. *J Am Acad Dermatol*. 2014;**70**(4):621–629.
42. Zheng ZM, Baker CC. Papillomavirus genome structure, expression, and post-transcriptional regulation. *Front Biosci*. 2006;**11**:2286–2302.
43. zur Hausen H. Papillomaviruses and cancer: from basic studies to clinical application. *Nat Rev Cancer*. 2002;**2**(5):342–350.